Available online at www.sciencedirect.com
SCIENCE DIRECT®
Journal of Sound and Vibration 273 (2004) 681–691
JOURNAL OF SOUND AND VIBRATION
www.elsevier.com/locate/jsvi

Letter to the Editor

Acoustic insulation provided by circular and infinite plane walls

Julieta António*, Luís Godinho, António Tadeu

Department of Civil Engineering, University of Coimbra, Pole II - Pinhal de Marrocos, 3030-290 Coimbra, Portugal

Received 17 February 2003; accepted 5 August 2003

1. Introduction

The transmission of sound energy is a complex phenomenon on account of the number and the interdependence of variables involved. In this context the mathematical modelling of this phenomenon becomes difficult. Of the models that have been developed, some of them only take a limited number of variables into account, leading to simplified models such as the Mass Law.

Among the simplified methods for evaluating the sound insulation provided by a single panel are those described by Sewell [1], Sharp [2], Cremer [3] and Callister et al. [4]. Novikov [5] used the mass law with the addition of a correction coefficient to study the sound insulation of finite plates, at low frequencies. Osipov et al. [6] studied the sound transmission through a single panel using an infinite plate model and a room–plate–room model. They noticed that at low frequencies the results are strongly influenced by the geometry and the dimensions of the room–wall–room system, in addition to the properties of the panel material.

Most of the articles published that take the full coupling between the fluid and the solid structure into account are restricted to low frequencies, because of the computational cost entailed, particularly when modelling closed spaces. This kind of analysis is simpler in the case of circular enclosures, for which analytical solutions can be derived.

Other authors in a different context have tackled the study of circular cylindrical shells. Veksler et al. [7] studied the modal resonances of submerged elastic circular cylindrical shells filled with air, when struck by plane harmonic acoustic waves. Their work used a standard resonance scattering theory, and paid special attention to the generation of bending waves. Bao et al. [8] analyzed the various circumferential waves generated when a circular cylindrical shell submerged in a fluid and filled with another fluid is disturbed by a normally incident plane wave. Maze et al. [9], in a related work, analyzed the existence of various guided acoustic circumferential modes in a water-filled tube.

*Corresponding author. Tel.: +351-239-797196; fax: +351-239-797190.
E-mail address: julieta@dec.uc.pt (J. António).

0022-460X/$ - see front matter
doi:10.1016/j.jsv.2003.08.028

The present work computes the acoustic sound insulation provided by circular structures surrounded and filled with air. The full coupling between the external fluid medium, the elastic material and the internal fluid medium is taken into account. The wall is assumed to have a constant cross section and is modelled as a homogeneous elastic material. The 3-D response is formulated in the frequency domain, and is obtained as a discrete summation of the 2-D solutions found for different axial wave numbers.

The sound insulation responses are compared with those obtained using the analytical model already proposed by the authors for an infinite plane wall [10] taking into account the coupling between the surrounding fluids and the elastic material of the wall.

The next section describes briefly the analytical solutions used to compute the pressure response of a circular structure and a plane wall bounded by air when subjected to a spatially sinusoidal harmonic line pressure load. After this, a number of applications are presented to illustrate the main features of the acoustic insulation obtained in the presence of a circular wall. Finally, different simulations are used to compare the sound insulation provided by the circular wall with that obtained for a plane wall.

2. Mathematical formulation

This section briefly describes the formulation of the analytical solutions for evaluating the acoustic behaviour of a circular wall and a plane wall of infinite extent.

2.1. Circular wall

A circular wall with internal and external radii, r_A and r_B respectively, is bounded by an inviscid compressible homogeneous air medium, as illustrated in Fig. 1. The wall is excited by a harmonic dilatational source placed in the fluid media.

Decomposing the homogeneous wave equations for elastic media in the usual way, by means of the now classical dilatational ϕ and shear potentials ψ, χ, one arrives at the three scalar wave equations (Helmholtz equations) in these potentials, with associated wave propagation velocities α, β and β respectively. For the fluid media the solution can be obtained by using the single dilatational potential ϕ_f, associated with the wave velocity α_f.

The 3-D incident field for a point pressure source, with frequency ω, placed at an off-centre position $(x_0, 0, 0)$ can be defined by means of the dilatational potential

$$\phi_{f\,inc}(\omega, r') = \left(\frac{-\alpha_f^2}{\omega^2 \lambda_f}\right) \frac{A e^{-i(\omega/\alpha_f)r'}}{r'} \tag{1}$$

with $r' = \sqrt{(x - x_0)^2 + y^2 + z^2}$, where the subscript *inc* refers to the incident field, A is the wave amplitude, r' is the distance between the source and the receiver, λ_f is the fluid Lamé constant, $\alpha_f = \sqrt{\lambda_f/\rho_f}$ and ρ_f are the acoustic (dilatational) wave velocity and the mass density of the fluid, respectively, and $i = \sqrt{-1}$. In this equation, a time dependence $e^{i\omega t}$ is implicit. The incident field can be expressed as a summation of 2-D sources, with different spatial wavenumbers, applying a

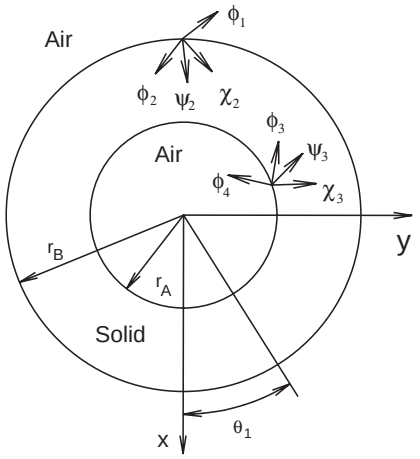

Fig. 1. Circular wall geometry and definition of the potentials.

Fourier transform along the z direction,

$$\phi_{f\ inc}(\omega, r') = \frac{2\pi}{L} \sum_{m=-M}^{M} \hat{\phi}_{f\ inc}(\omega, r'', k_{zm}) \mathrm{e}^{-\mathrm{i}k_{zm}z} \tag{2}$$

with $\hat{\phi}_{f\ inc}(\omega, r'', k_{zm}) = -\frac{1}{2}\mathrm{i}A(-\alpha_f^2/(\omega^2\lambda_f))H_0^{(2)}(k_{\alpha_f} r'')$, $r'' = \sqrt{(x-x_0)^2 + y^2}$, $k_{\alpha f} = \sqrt{\omega^2/\alpha_f^2 - k_{zm}^2}$ ($\mathrm{Im}\, k_{\alpha f} < 0$), $k_{\alpha_f} = \sqrt{\omega^2/\alpha_f^2 - k_{zm}^2}$, k_{zm} being the axial wavenumber given by $k_{zm} = (2\pi/L)m$, $H_n^{(2)}(\ldots)$ the second Hankel functions of order n, and L the distance between virtual point sources equally spaced along z.

The wavefield in the exterior fluid medium corresponds to diverging or outgoing waves, and they can be represented by Hankel functions of second type and order n.

$$\phi_1(\omega, r, k_{zm}) = \sum_{n=0}^{\infty} A_n^1 H_n^{(2)}(k_{\alpha_f} r) \cos(n\theta_1), \tag{3}$$

where A_n^1 is an unknown potential amplitude.

The waves propagating inside the elastic material of the circular wall correspond to inward travelling waves, generated at the external surface, and to outward travelling waves, generated at the internal surface of the wall. These waves can be described by two dilatational and four shear potentials (see Fig. 1).

$$\phi_2(\omega, r, k_{zm}) = \sum_{n=0}^{\infty} A_n^2 J_n(k_\alpha r) \cos(n\theta_1), \quad \phi_3(\omega, r, k_{zm}) = \sum_{n=0}^{\infty} A_n^5 H_n^{(2)}(k_\alpha r) \cos(n\theta_1),$$

$$\psi_2(\omega, r, k_{zm}) = \sum_{n=0}^{\infty} A_n^3 J_n(k_\beta r) \sin(n\theta_1), \quad \psi_3(\omega, r, k_{zm}) = \sum_{n=0}^{\infty} A_n^6 H_n^{(2)}(k_\beta r) \sin(n\theta_1),$$

$$\chi_2(\omega, r, k_{zm}) = \sum_{n=0}^{\infty} A_n^4 J_n(k_\beta r) \cos(n\theta_1), \quad \chi_3(\omega, r, k_{zm}) = \sum_{n=0}^{\infty} A_n^7 H_n^{(2)}(k_\beta r) \cos(n\theta_1) \tag{4}$$

with $k_\alpha = \sqrt{\omega^2/\alpha^2 - k_{zm}^2}$, $k_\beta = \sqrt{\omega^2/\beta^2 - k_{zm}^2}$ and A_n^2, A_n^3, A_n^4, A_n^5, A_n^6 and A_n^7 are unknown potential amplitudes.

In the inner fluid, the wavefield consists of waves coming from the internal surface of the wall, defined by the dilatational potential (see Fig. 1),

$$\phi_4(\omega, r, k_{zm}) = \sum_{n=0}^{\infty} A_n^8 J_n(k_{\alpha_f} r)\cos(n\theta_1), \tag{5}$$

where A_n^8 is an unknown potential amplitude.

The unknown coefficients A_n^j ($j = 1, 8$) are determined by imposing the required boundary conditions, which are the continuity of normal displacements and normal stresses and null tangential stresses, on the two solid–fluid interfaces. The acoustic insulation provided by the circular wall is found from the difference between the pressures registered at receivers placed at both sides of the wall.

2.2. Plane wall of infinite extent

The model assumes the existence of a solid layer formation, with thickness h, bounded by two external fluid media, excited by a spatially sinusoidal harmonic pressure load along the z direction, with frequency ω, acting at the point (x_0, y_0) in the top fluid medium (see Fig. 2).

The technique uses solid displacement potentials and fluid pressure potentials expressed as a superposition of plane waves, with different wavenumbers, k_n, along the x direction. The problem is formulated assuming the existence of an infinite number of virtual loads distributed along the x direction, at equal intervals L_x, permitting the definition of $k_n = (2\pi/L_x)n$. The distance L_x needs to be large enough to prevent the virtual loads contaminating the response.

The solution can be defined as the sum of the incident wave field in an unbounded medium with a set of surface terms defined so as to satisfy the continuity of normal displacements and stresses and null tangential stresses conditions at the fluid–solid interfaces. Each solid–fluid interface generates surface terms, which can be expressed as the sum of shear and dilatational potentials (see Fig. 2).

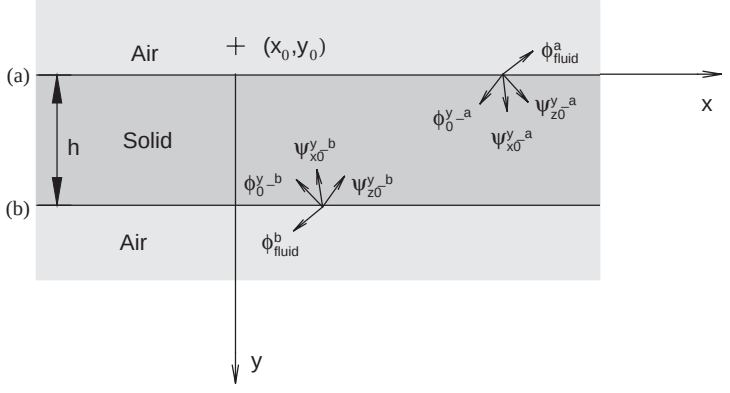

Fig. 2. Plane wall geometry and definition of the potentials.

The amplitude of these potentials can be obtained from the appropriate boundary conditions, so that the field produced simultaneously by the source and surface terms leads to null shear stress and the continuity of normal displacements and stresses at the solid–fluid interfaces. A full description of this solution can be found in Ref. [10].

3. Numerical applications

The above expressions were used to compute the acoustic insulation provided by a circular and a flat wall, after the calculation of the pressure amplitude on both sides of the wall, when a harmonic line pressure load with a spatial sinusoidal variation disturbs these dynamic systems.

In our examples, different thicknesses (h) were ascribed to a concrete wall. The internal material loss is introduced using a complex Young's modulus and complex Lamé constants. The Young's modulus is expressed as $E = E_r(1 + i\xi)$, where E_r corresponds to the classic modulus and ξ is the loss factor. The complex Lamé constants can be written in the same form as the Young's modulus.

The fluid medium (air) surrounding the wall allows a pressure wave velocity of $\alpha_f = 340$ m/s and a density of $\rho_f = 1.22$ kg/m^3. The properties of the solid wall material are listed in Table 1.

The acoustic insulation computations are performed with a frequency increment of 1 Hz, from 1 to 6000 Hz. A selection of results is given below to illustrate the main findings of the present work. First, a closed circular concrete wall is used to illustrate how the acoustic insulation changes when subjected to line sources ($k_z = 0$) placed either on or off the axis of the circular wall. Insulation curves for different wall thicknesses and curvatures are included. Afterwards, a set of simulations compares the insulation given by a circular wall and a plane wall.

3.1. Insulation responses of a circular closed wall

In the first example, a circular, closed, concrete wall (with an interior radius of $r_A = 5.0$ m), 0.30 m thick, is subjected to a line pressure load ($k_z = 0$) placed at its centre ($d = 0$ m). The pressure is registered over three circular lines of 16 receivers placed on either side of the wall, 0.5, 1.0 and 1.5 m away from the inner and outer surfaces of the wall (see Fig. 3). As the source is central, the amplitude is the same at each curved line of receivers.

Fig. 4a shows the amplitude of the frequency responses recorded at receivers R1 and R2, placed 0.5 m from the wall, outside and inside the enclosure (as in Fig. 3). Both curves exhibit pronounced peaks, which were identified as being coincident with the first (axisymmetric) normal modes generated within the air inside the circular wall. The eigenfrequencies associated with these modes have been defined assuming that the air is limited by a rigid structure. When this boundary condition is applied, the expression $(n/r)J_n(k_{\alpha_f} r) - k_{\alpha_f} J_{n+1}(k_{\alpha_f} r) = 0$ is defined, which allows the

Table 1
Material properties

Material	Shear modulus (GPa)	Modulus of elasticity (GPa)	Poisson ratio	Density (kg/m^3)	α (m/s)	β (m/s)	Loss factor (ξ)
Concrete	12.6	28.98	0.15	2500	3498.6	2245	6×10^{-3}

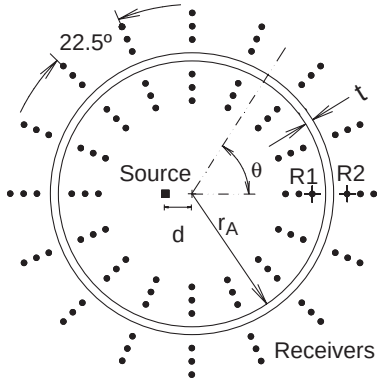

Fig. 3. Position of the receivers and sources in the circular wall model.

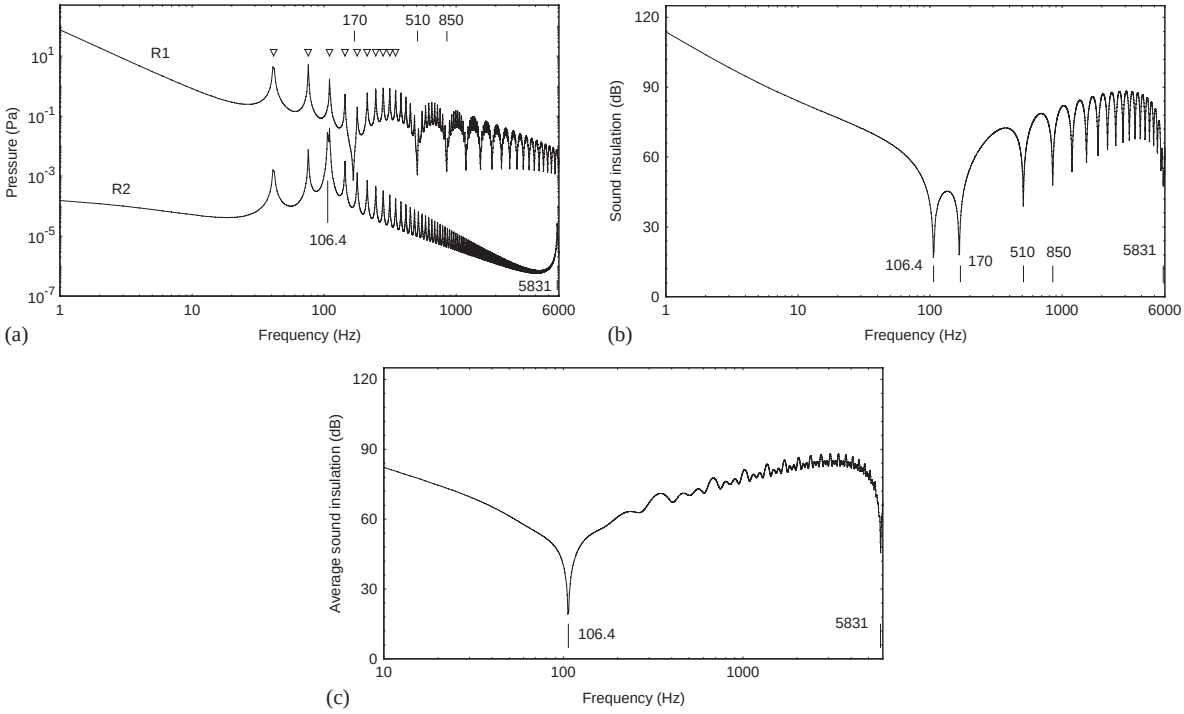

Fig. 4. Computation in the presence of a 0.30 m thick circular concrete wall with an inner radius of $r_A = 5.0$ m, when subjected to a cylindrical line source ($k_z = 0$) placed on the axis: (a) amplitude pressure response registered at receivers R1 and R2, placed 0.5 m from the wall; (b) acoustic insulation obtained by the difference between the responses at R1 and R2; (c) average insulation obtained for the full grid of receivers.

position of these modes to be identified. In the particular case of a source placed on the axis of the circular wall, the solution is only given when $n = 0$ has been ascribed to this equation, to give $J_1(k_{\alpha_f} r) = 0$. Fig. 4a includes the first positions of these modes (triangular marks), which agree with the location of the frequency response peaks.

The response at receiver R2 shows an additional peak at frequency 106.4 Hz that corresponds to the first axisymmetric mode of the solid structure (circular wall). The position of these natural modes can be evaluated, assuming that the circular wall has free inner and outer surfaces. The stresses within the circular wall are derived using the potentials given by Eqs. (4). The solution of this problem is established by imposing null stresses along the inner and outer surfaces of the wall that leads to the final system of equations $[\mathbf{K}][\mathbf{X}] = [\mathbf{0}]$. The response is other than zero if the determinant $|\mathbf{K}|$ is set to be zero. The solution of the resulting equation gives the required position of the natural modes. Again, when the source is placed on the axis, only the axisymmetric modes are excited, which corresponds to $n = 0$.

The response registered at receiver R2 exhibits an additional peak at high frequencies, associated with the wave resonance within the panel thickness ($f = \alpha/(2h) = 5831$ Hz).

The amplitude response at receiver R1 shows well-defined dips, resulting from the interaction between the direct incident pulses with the reflected pulses. This occurs when the difference between these path lengths Δs is a multiple of the wavelength ($0.5\alpha_f/\Delta s = 170$ Hz, $1.5\alpha_f/\Delta s = 510$ Hz, $2.5\alpha_f/\Delta s = 850$ Hz, etc.). Note that the position of these dips varies according to the receiver location.

Fig. 4b displays the insulation curve, provided by the difference between the amplitudes of the previous curves, in a dB scale. In this curve, a set of dips can be observed. The first dip corresponds to the first axisymmetric mode of the wall as detected at receiver R2. The other dips, as mentioned before, appear as a result of the interaction of the incident wave field with the directly reflected field and at high frequencies associated with the resonance effect within the wall thickness.

Fig. 4c displays the average insulation curve obtained from the pressure responses registered along all the lines of receivers, on a dB scale. As the contribution of 48 receivers in each side of the wall is taken into account, the influence of the interaction between incident and reflected pulses is now less evident, and only pronounced dips related to the axisymmetric mode of the wall and with the resonance effect within the wall thickness are present.

Next, the same wall is excited by an off-centre source placed so that $d = 1.0$ m (see Fig. 3). The average sound insulation, calculated with the full set of receivers, is illustrated in Fig. 5. The curve now has a more complex pattern than that observed when the source was placed on the axis. The complexity is due to the interaction between the incident and the reflected waves within the enclosure, the vibration modes of the wall structure and the resonances within the fluid trapped in the circular closed wall. When the source is not central, non-axisymmetric modes of the fluid inside the wall, and of the wall structure, are excited. These modes are defined as explained above, by ascribing to n values of 0, 1, 2, etc. This plot marks the first modes associated with the wave resonances within the fluid, and it can be observed that both responses exhibit dips at these positions. The position of the first eigenfrequencies, related to the solid wall eigenmodes, is indicated on this plot with small ticks. It can be seen that the response exhibits oscillations that testify to the excitation of these modes. As before, a dip related to the resonance frequency inside the wall thickness is visible ($f = \alpha/(2h) = 5831$ Hz).

The effect of the wall thickness on the sound insulation is assessed next. Fig. 6 plots the average sound insulation provided by circular concrete walls, with the same internal radius of $r_A = 5.0$ m, but with different thicknesses, $t = 0.15$, 0.30 and 0.40 m, when the source is placed on the axis. All insulation curves exhibit a well-pronounced dip in the vicinity of the natural vibration of the solid

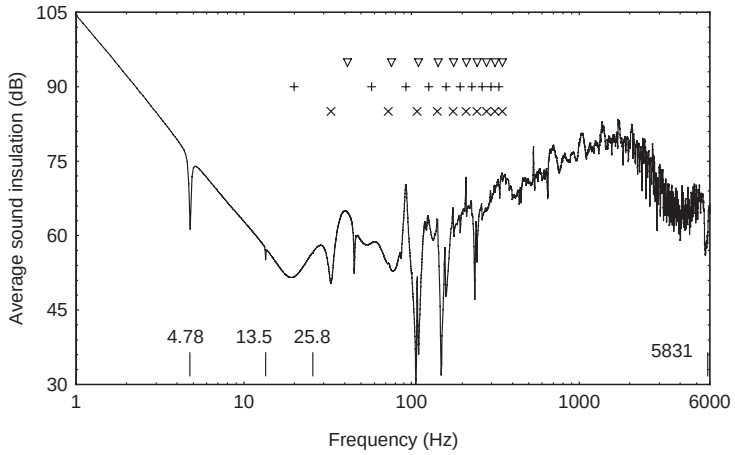

Fig. 5. Average insulation obtained in the presence of a 0.30 m thick circular concrete wall with an inner radius $r_A = 5.0$ m, when subjected to a cylindrical line source ($k_z = 0$) placed at an off centre position ($d = 1.0$ m).

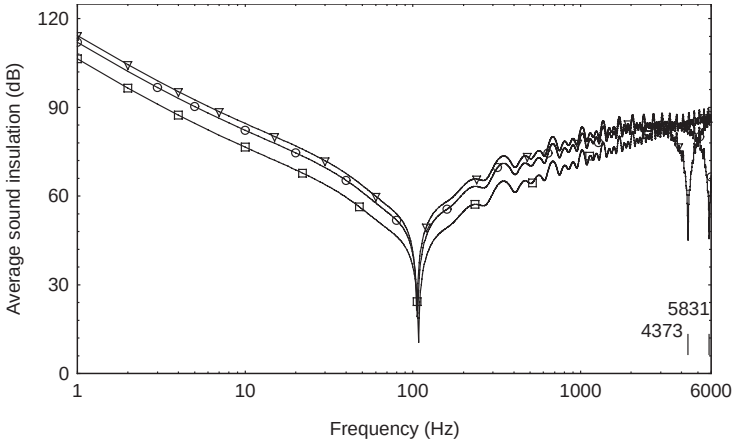

Fig. 6. Computed average insulation curves for a circular concrete wall, with an inner radius $r_A = 5.0$ m, subjected to a cylindrical line source ($k_z = 0$), placed on the axis, for thicknesses $t = 0.15$ m (□), $t = 0.30$ m (○) and $t = 0.40$ m (▽).

wall, located at $f = 108.0$, 106.4 and 105.4 Hz when the wall changes from being 0.15 m thick (t) to 0.30 m and then $t = 0.40$ m thick. As expected, the sound insulation increases as the thickness increases, particularly at lower frequencies. However, this difference is less evident for higher frequencies and it is highly affected by the resonance within the wall. Notice that as the wall becomes thicker this insulation dip appears at lower frequencies.

Fig. 7 illustrates the sound insulation provided by the 0.30 m thick concrete wall, when the inner radius varies, while the source remains at the centre of the enclosure. The influence of the dimensions of the enclosure is more evident for low frequencies, where the sound insulation diminishes with increasing radius curvature. This is, particularly affected by the first eigenmode of the solid structure, which occurs at $f = 5.5$, 13.6 and 106.4 Hz, when the inner radius of the wall

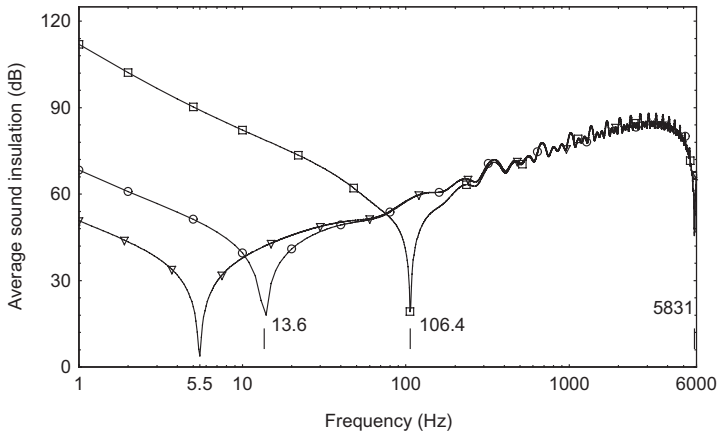

Fig. 7. Computed insulation curves for a 0.30 m thick concrete wall when subjected to a cylindrical line source ($k_z = 0$), placed on the axis, with inner radii $r_A = 5.0$ m (□), $r_A = 40.0$ m (○) and $r_A = 100.0$ m (▽).

(r_A) is first 100.0 m, then 40.0 m and then 5.0 m. The acoustic insulation provided by these three different walls converges as the frequency increases.

3.2. Insulation provided by a circular closed wall versus a plane wall

In the next examples the sound insulation provided by a circular wall is compared with that obtained for a plane wall of infinite extent. All the walls are 0.30 m thick, made of concrete, and the source in the circular wall is at the centre. The radius of the circular wall is assumed to vary from $r_A = 5.0$ to 100.0 m. The computations performed for the plane wall assume that a line pressure source ($k_z = 0$) is placed at the same distance from the wall as in the case of the circular wall: in the first case $e = 5.0$ m from the wall, and in the second case $e = 100.0$ m from the wall's surface. The response is calculated along a grid of receivers, placed on either side of the wall, as shown in Fig. 8a.

Fig. 8b shows the average sound insulation obtained when the radius r_A is 5.0 m. The curve obtained for the plane wall exhibits dips in the insulation, associated with the coincidence effect and with the resonance inside the wall thickness. The sound insulation curve obtained for a circular wall shows dips related to the first vibrational mode of the wall and to the resonance inside the wall thickness, as mentioned above. It happens that in the case of a circular wall the receivers do not record the presence of the guided waves when the source is a line pressure load ($k_z = 0$), and on the axis. It can be observed that the sound insulation provided by the circular wall differs from that provided by the plane wall, mainly for low frequencies, where the circular wall confers higher insulation, given the rigidity of the closed wall. Fig. 8c shows the average sound insulation when the source is 100.0 m from the surface of a wall. In this case, as the source is a long way from the plane wall, the waves reaching its surface behave similarly to plane waves, leading to the weakness of the coincidence effect. These two insulation curves are closer than before, especially above the eigenfrequency associated with the first mode of the circular wall. For high frequencies the sound insulation obtained for the plane wall suffers a drop, owing to the interference of guided waves travelling along the wall.

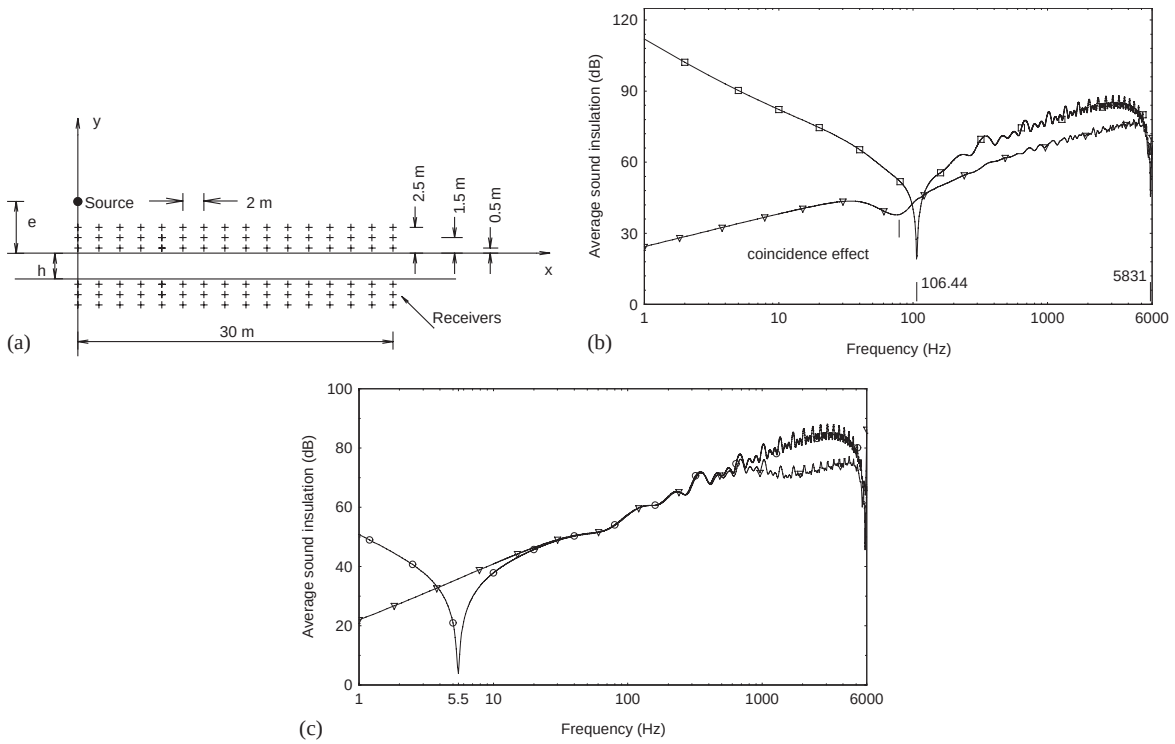

Fig. 8. Insulation provided by a circular closed wall versus a plane wall 0.30 m thick, made of concrete: (a) Position of the receivers and sources for the plane wall model. (b) Average sound insulation obtained when the radius of the circular wall $r_A = 5.0$ m (□—circular wall $r_A = 5.0$ m; ▽—plane wall). The source is placed on the axis in the case of the circular wall, whereas it is $e = 5.0$ m away from the plane wall. (c) Average sound insulation obtained when the radius of the circular wall $r_A = 100.0$ m (○—circular wall, $r_A = 100.0$ m; ▽—plane wall). The source is placed on the axis in the case of the circular wall, whereas it is $e = 100.0$ m away from the plane wall.

4. Conclusions

Analytical solutions have been used for the calculation of the acoustic insulation provided by single circular and plane walls, when subjected to a spatially sinusoidal harmonic line pressure load.

The calculated responses show that the sound insulation provided by a circular wall is highly dependent on the vibration modes excited in the inner fluid, and on the way the solid wall vibrates. In the vicinity of these eigenfrequencies the insulation exhibits pronounced dips. Besides these dips, the synthetic signals reveal the presence of a complicated wavefield, generated by both body waves and the guided surface waves that travel around the circular wall when the source is off axis.

The average insulation calculated for the different circular wall thicknesses increases, at frequencies not associated with the resonance effects, with increasing wall thickness. The computed insulation provided by circular walls with the same thickness and differing inner radius is markedly different at low frequencies, while its behaviour approaches that at high frequencies.

The acoustic insulation obtained for a circular wall approaches that of a plane wall, beyond the natural vibration frequency of the solid wall structure only if the inner radius of the circular wall is very large. The coincidence effect observed for plane walls was not observed in the simulations for the circular wall. It would require a larger inner radius and the source to be placed off center.

References

[1] E.C. Sewell, Transmission of reverberant sound through a single-leaf partition surrounded by an infinite rigid baffle, *Journal of Sound and Vibration* 12 (1970) 21–32.
[2] B.H. Sharp, Prediction methods for the sound transmission of building elements, *Noise Control Engineering* 11 (1978) 53–63.
[3] L. Cremer, Theorie der Shalldämmung dünner Wände bei schrägem Einfall, *Akustische Zeitschrift* 7 (1942) 81–102.
[4] J.R. Callister, A.R. George, G.E. Freeman, An empirical scheme to predict the sound transmission loss of single-thickness panels, *Journal of Sound and Vibration* 222 (1999) 145–151.
[5] I. Novikov, Low-frequency sound insulation of thin plates, *Applied Acoustics* 54 (1998) 83–90.
[6] A. Osipov, P. Mees, G. Vermeir, Low-frequency airborne sound transmission through single partitions in buildings, *Applied Acoustics* 52 (1997) 273–288.
[7] N. Veksler, J. Izbicki, J. Conoir, Bending A wave in the scattering by a circular cylindrical shell: its relation with the bending free modes, *Journal of the Acoustical Society of America* 96 (1994) 287–293.
[8] X.L. Bao, P.K. Raju, H. Uberall, Circumferential waves on an immersed, fluid-filled elastic cylindrical shell, *Journal of the Acoustical Society of America* 105 (1999) 2704–2709.
[9] G. Maze, J. Cheeke, X. Li, Z. Wang, Coupled guided acoustic modes in water-filled thin-walled tubes, *Journal of the Acoustical Society of America* 110 (2001) 2295–2300.
[10] A. Tadeu, J. António, Acoustic insulation of single panel walls provided by analytical expressions versus the mass law, *Journal of Sound and Vibration* 257 (3) (2002) 457–475.